

# Direct photons as probes of low mass strings at the LHC

Luis A. Anchordoqui,<sup>1</sup> Haim Goldberg,<sup>2</sup> Satoshi Nawata,<sup>1</sup> and Tomasz R. Taylor<sup>2</sup>

<sup>1</sup>*Department of Physics,  
University of Wisconsin-Milwaukee, Milwaukee, WI 53201, USA*

<sup>2</sup>*Department of Physics,  
Northeastern University, Boston, MA 02115, USA*

(Dated: April 2008)

## Abstract

The LHC program will include the identification of events with single prompt high- $k_{\perp}$  photons as probes of new physics. We show that this channel is uniquely suited to search for experimental evidence of TeV-scale open string theory. At the parton level, we analyze single photon production in gluon fusion,  $gg \rightarrow \gamma g$ , with open string states propagating in intermediate channels. If the photon mixes with the gauge boson of the baryon number, which is a common feature of D-brane quivers, the amplitude appears already at the string disk level. It is completely determined by the mixing parameter (which is actually determined in the minimal theory) – and it is otherwise model-(compactification-) independent. We discuss the string signal cross sections as well as the QCD background. The present analysis takes into account the recently obtained decay widths of first Regge recurrences, which are necessary for more precise determination of these cross sections in the resonant region. A vital part of the background discussion concerns the minimization of misidentified  $\pi^0$ 's emerging from high- $p_{\perp}$  jets. We show that even for relatively small mixing, 100 fb<sup>-1</sup> of LHC data could probe deviations from standard model physics associated with TeV-scale strings at a  $5\sigma$  significance, for  $M_{\text{string}}$  as large as 2.3 TeV. It is also likely that resonant bumps could be observed with approximately the same signal-to-noise ratio.

## I. GENERAL IDEA

The CERN's Large Hadron Collider (LHC) is the greatest basic science endeavor in history. Spectacular physics results are expected to follow in short order once it turns on this year. LHC will push nucleon-nucleon center-of-mass energies up to  $\sqrt{s} = 14$  TeV for  $pp$  collisions and  $\sqrt{s} = 5.5$  TeV for Pb-Pb collisions. The ATLAS and CMS detectors will observe the highest-energy particle collisions produced by the accelerator, whereas the ALICE detector will observe the very messy debris of heavy ion collisions. The LHC will probe deeply into the sub-fermi distances, committing to careful searches for new particles and interactions at the TeV scale.

At the time of its formulation and for years thereafter, Superstring Theory was regarded as a unifying framework for Planck-scale quantum gravity and TeV-scale Standard Model (SM) physics. Important advances were fueled by the realization of the vital role played by D-branes [1] in connecting string theory to phenomenology [2]. This has permitted the formulation of string theories with compositeness setting in at TeV scales [3] and large extra dimensions. There are two paramount phenomenological consequences for TeV scale D-brane string physics: the emergence of Regge recurrences at parton collision energies  $\sqrt{\hat{s}} \sim \text{string scale} \equiv M_s$ ; and the presence of one or more additional  $U(1)$  gauge symmetries, beyond the  $U(1)_Y$  of the SM. The latter follows from the property that the gauge group for open strings terminating on a stack of  $N$  identical D-branes is  $U(N)$  rather than  $SU(N)$  for  $N > 2$ . (For  $N = 2$  the gauge group can be  $Sp(1)$  rather than  $U(2)$ .) In this paper we exploit both these properties in order to obtain a “new physics” signal at LHC which, if traced to low scale string theory, could with  $100 \text{ fb}^{-1}$  of data probe deviations from SM physics at a  $5\sigma$  significance for  $M_s$  as large as 2.3 TeV. A short version highlighting the salient results of our analysis has been issued as a companion Letter [4]. The present analysis, however, takes into account the recently obtained decay widths of first Regge recurrences [5], which are necessary for more precise determination of cross sections in the resonant region.

To develop our program in the simplest way, we will work within the construct of a minimal model in which we consider scattering processes which take place on the (color)  $U(3)$  stack of D-branes. In the bosonic sector, the open strings terminating on this stack contain, in addition to the  $SU(3)$  octet of gluons, an extra  $U(1)$  boson ( $C_\mu$ , in the notation of [6]), most simply the manifestation of a gauged baryon number symmetry. The  $U(1)_Y$  boson  $Y_\mu$ , which gauges the usual electroweak hypercharge symmetry, is a linear combination of  $C_\mu$ , the  $U(1)$  boson  $B_\mu$  terminating on a separate  $U(1)$  brane, and perhaps a third additional  $U(1)$  (say  $W_\mu$ ) sharing a  $U(2)$  brane to which are also a terminus for the  $SU(2)_L$  electroweak gauge bosons  $W_\mu^a$ . Thus, critically for our purposes, the photon  $A_\mu$ , which is a linear combination of  $Y_\mu$  and  $W_\mu^3$  *will participate with the gluon octet in (string) tree level scattering processes on the color brane, processes which in the SM occur only at one-loop level.* Such a mixing between hypercharge and baryon number is a generic property of D-brane quivers, see *e.g.* Refs.[6, 7, 8]. The vector boson  $Z'_\mu$ , orthogonal to the hypercharge, must grow a mass  $M_{Z'}$  in order to avoid long range forces between baryons other than gravity and Coulomb forces.

The process we consider (at the parton level) is  $gg \rightarrow g\gamma$ , where  $g$  is an  $SU(3)$  gluon and  $\gamma$  is the photon. As explicitly calculated below, this will occur at string disk (tree) level, and will be manifest at LHC as a non-SM contribution to  $pp \rightarrow \gamma + \text{jet}$ . A very important property of string disk amplitudes is that they are completely model-independent; thus the results presented below are robust, because *they hold for arbitrary compactifications of superstring theory from ten to four dimensions, including those that break super-*

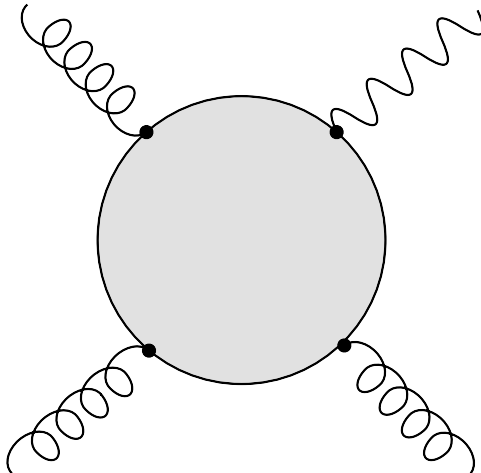


FIG. 1: Open string disk diagram for  $gg \rightarrow g\gamma$  scattering. The dots represent vertex insertions of the gauge bosons on the boundary of the world sheet.

*symmetry.* The SM background for this signal originates in the parton tree level processes  $gq \rightarrow \gamma q$ ,  $g\bar{q} \rightarrow \gamma\bar{q}$ , and  $q\bar{q} \rightarrow \gamma g$ . Of course, the SM processes will also receive stringy corrections which should be added to the pure bosonic contribution as part of the signal [9, 10, 11, 12]. We leave this evaluation to a subsequent publication [13]; thus, the contribution from the bosonic process calculated here is to be regarded as a lower bound to the stringy signal. It should also be stated that, in what follows, we do not include effects of Kaluza-Klein recurrences due to compactification. We assume that all such effects are in the gravitational sector, and hence occur at higher order in string coupling [9].

The plan of the paper is as follows. In the next section we outline the calculation of the string amplitude for the process pictured in Fig. 1 and show that there is no amplitude containing the zero mass poles of the SM. In Sec. III we first calculate cross sections for gluon fusion in the resonance region as well as QCD background, for a simple  $k_{\perp,\min}$  cut on the transverse momentum of the photon. A vital part of the background discussion concerns the minimization of misidentified  $\pi^0$ 's from high- $p_{\perp}$  jets. After that we calculate the signal-to-noise ratio and show that a significant deviation from SM can be obtained for  $k_{\perp,\min} > 300$  GeV for  $M_s$  as large as 2.3 TeV. In Sec. IV we delineate the search for resonant structure in the data. Our conclusions are collected in Sec. V. The Appendices contain some additional formulae referred to in the main text.

## II. THE STRING AMPLITUDE

The most direct way to compute the amplitude for the scattering of four gauge bosons is to consider the case of polarized particles because all non-vanishing contributions can be then generated from a single, maximally helicity violating (MHV), amplitude – the so-called *partial* MHV amplitude [14]. Assume that two vector bosons, with the momenta  $k_1$  and  $k_2$ , in the  $U(N)$  gauge group states corresponding to the generators  $T^{a_1}$  and  $T^{a_2}$  (here in the fundamental representation), carry negative helicities while the other two, with the momenta  $k_3$  and  $k_4$  and gauge group states  $T^{a_3}$  and  $T^{a_4}$ , respectively, carry positive helicities. (All momenta are incoming.) Then the partial amplitude for such an MHV configuration is given

by [15, 16]

$$A(1^-, 2^-, 3^+, 4^+) = 4g^2 \text{Tr}(T^{a_1} T^{a_2} T^{a_3} T^{a_4}) \frac{\langle 12 \rangle^4}{\langle 12 \rangle \langle 23 \rangle \langle 34 \rangle \langle 41 \rangle} V(k_1, k_2, k_3, k_4), \quad (1)$$

where  $g$  is the  $U(N)$  coupling constant,  $\langle ij \rangle$  are the standard spinor products written in the notation of Refs. [17, 18], and the Veneziano formfactor,

$$V(k_1, k_2, k_3, k_4) = V(s, t, u) = \frac{\Gamma(1-s) \Gamma(1-u)}{\Gamma(1+t)}, \quad (2)$$

is the function of Mandelstam variables, here normalized in the string units:

$$s = \frac{2k_1 k_2}{M_s^2}, \quad t = \frac{2k_1 k_3}{M_s^2}, \quad u = \frac{2k_1 k_4}{M_s^2} : \quad s + t + u = 0. \quad (3)$$

(For simplicity we drop carets for the parton subprocess.) Its low-energy expansion reads

$$V(s, t, u) \approx 1 - \frac{\pi^2}{6} s u - \zeta(3) s t u + \dots \quad (4)$$

We first consider the amplitude involving three  $SU(N)$  gluons  $g_1, g_2, g_3$  and one  $U(1)$  gauge boson  $\gamma_4$  associated to the same  $U(N)$  quiver:

$$T^{a_1} = T^a, \quad T^{a_2} = T^b, \quad T^{a_3} = T^c, \quad T^{a_4} = QI, \quad (5)$$

where  $I$  is the  $N \times N$  identity matrix and  $Q$  is the  $U(1)$  charge of the fundamental representation. The  $U(N)$  generators are normalized according to

$$\text{Tr}(T^a T^b) = \frac{1}{2} \delta^{ab}. \quad (6)$$

Then the color factor

$$\text{Tr}(T^{a_1} T^{a_2} T^{a_3} T^{a_4}) = Q(d^{abc} + \frac{i}{4} f^{abc}), \quad (7)$$

where the totally symmetric symbol  $d^{abc}$  is the symmetrized trace while  $f^{abc}$  is the totally antisymmetric structure constant.

The full MHV amplitude can be obtained [15, 16] by summing the partial amplitudes (1) with the indices permuted in the following way:

$$\mathcal{M}(g_1^-, g_2^-, g_3^+, \gamma_4^+) = 4g^2 \langle 12 \rangle^4 \sum_{\sigma} \frac{\text{Tr}(T^{a_{1\sigma}} T^{a_{2\sigma}} T^{a_{3\sigma}} T^{a_4}) V(k_{1\sigma}, k_{2\sigma}, k_{3\sigma}, k_4)}{\langle 1_{\sigma} 2_{\sigma} \rangle \langle 2_{\sigma} 3_{\sigma} \rangle \langle 3_{\sigma} 4 \rangle \langle 41_{\sigma} \rangle}, \quad (8)$$

where the sum runs over all 6 permutations  $\sigma$  of  $\{1, 2, 3\}$  and  $i_{\sigma} \equiv \sigma(i)$ . Note that in the effective field theory of gauge bosons there are no Yang-Mills interactions that could generate this scattering process at the tree level. Indeed,  $V = 1$  at the leading order of Eq.(4) and the amplitude vanishes due to the following identity:

$$\frac{1}{\langle 12 \rangle \langle 23 \rangle \langle 34 \rangle \langle 41 \rangle} + \frac{1}{\langle 23 \rangle \langle 31 \rangle \langle 14 \rangle \langle 42 \rangle} + \frac{1}{\langle 31 \rangle \langle 12 \rangle \langle 24 \rangle \langle 43 \rangle} = 0. \quad (9)$$

Similarly, the antisymmetric part of the color factor (7) cancels out in the full amplitude (8). As a result, one obtains:

$$\mathcal{M}(g_1^-, g_2^-, g_3^+, \gamma_4^+) = 8Q d^{abc} g^2 \langle 12 \rangle^4 \left( \frac{\mu(s, t, u)}{\langle 12 \rangle \langle 23 \rangle \langle 34 \rangle \langle 41 \rangle} + \frac{\mu(s, u, t)}{\langle 12 \rangle \langle 24 \rangle \langle 13 \rangle \langle 34 \rangle} \right), \quad (10)$$

where

$$\mu(s, t, u) = \Gamma(1-u) \left( \frac{\Gamma(1-s)}{\Gamma(1+t)} - \frac{\Gamma(1-t)}{\Gamma(1+s)} \right). \quad (11)$$

All non-vanishing amplitudes can be obtained in a similar way. In particular,

$$\mathcal{M}(g_1^-, g_2^+, g_3^-, \gamma_4^+) = 8Q d^{abc} g^2 \langle 13 \rangle^4 \left( \frac{\mu(t, s, u)}{\langle 13 \rangle \langle 24 \rangle \langle 14 \rangle \langle 23 \rangle} + \frac{\mu(t, u, s)}{\langle 13 \rangle \langle 24 \rangle \langle 12 \rangle \langle 34 \rangle} \right), \quad (12)$$

and the remaining ones can be obtained either by appropriate permutations or by complex conjugation.

In order to obtain the cross section for the (unpolarized) partonic subprocess  $gg \rightarrow g\gamma$ , we take the squared moduli of individual amplitudes, sum over final polarizations and colors, and average over initial polarizations and colors. As an example, the modulus square of the amplitude (8) is:

$$|\mathcal{M}(g_1^-, g_2^-, g_3^+, \gamma_4^+)|^2 = 64Q^2 d^{abc} d^{abc} g^4 \left| \frac{s\mu(s, t, u)}{u} + \frac{s\mu(s, u, t)}{t} \right|^2. \quad (13)$$

Taking into account all  $4(N^2 - 1)^2$  possible initial polarization/color configurations and the formula [19]

$$\sum_{a,b,c} d^{abc} d^{abc} = \frac{(N^2 - 1)(N^2 - 4)}{16N}, \quad (14)$$

we obtain the average squared amplitude

$$|\mathcal{M}(gg \rightarrow g\gamma)|^2 = g^4 Q^2 C(N) \left\{ \left| \frac{s\mu(s, t, u)}{u} + \frac{s\mu(s, u, t)}{t} \right|^2 + (s \leftrightarrow t) + (s \leftrightarrow u) \right\}, \quad (15)$$

where

$$C(N) = \frac{2(N^2 - 4)}{N(N^2 - 1)}. \quad (16)$$

The two most interesting energy regimes of  $gg \rightarrow g\gamma$  scattering are far below the string mass scale  $M_s$  and near the threshold for the production of massive string excitations. At low energies, Eq. (15) becomes

$$|\mathcal{M}(gg \rightarrow g\gamma)|^2 \approx g^4 Q^2 C(N) \frac{\pi^4}{4} (s^4 + t^4 + u^4) \quad (s, t, u \ll 1). \quad (17)$$

The absence of massless poles, at  $s = 0$  *etc.*, translated into the terms of effective field theory, confirms that there are no exchanges of massless particles contributing to this process. On the other hand, near the string threshold  $s \approx M_s^2$  (where we now restore the string scale)

$$|\mathcal{M}(gg \rightarrow g\gamma)|^2 \approx 4g^4 Q^2 C(N) \frac{M_s^8 + t^4 + u^4}{M_s^4 (s - M_s^2)^2} \quad (s \approx M_s^2). \quad (18)$$

The singularity at  $s = M_s^2$  needs softening to a Breit-Wigner form, reflecting the finite decay widths of resonances propagating in the  $s$  channel. Due to averaging over initial polarizations, Eq.(18) contains additively contributions from both spin  $J = 0$  and spin  $J = 2$  gluonic Regge recurrences ( $G^*$  in the notation of Ref.[5]), created by the incident gluons in the helicity configurations  $(\pm\pm)$  and  $(\pm\mp)$ , respectively. The  $M_s^8$  term in Eq. (18) originates from  $J = 0$ , and the  $t^4 + u^4$  piece reflects  $J = 2$  activity. Since the resonance widths are spin-dependent [5]:

$$\begin{aligned}\Gamma^{J=0} &= \frac{3}{4}\alpha_s M_s \approx 75 (M_s/\text{TeV}) \text{ GeV} , \\ \Gamma^{J=2} &= \frac{9}{20}\alpha_s M_s \approx 45 (M_s/\text{TeV}) \text{ GeV} ,\end{aligned}\tag{19}$$

the pole term (18) should be smeared as

$$|\mathcal{M}(gg \rightarrow g\gamma)|^2 \simeq \frac{4g^4 Q^2 C(N)}{M_s^4} \left[ \frac{M_s^8}{(s - M_s^2)^2 + (\Gamma^{J=0} M_s)^2} + \frac{t^4 + u^4}{(s - M_s^2)^2 + (\Gamma^{J=2} M_s)^2} \right]. \tag{20}$$

In what follows we will take  $N = 3$  and set  $g$  equal to the QCD coupling constant,  $\alpha_s = (g^2/4\pi) \sim 0.1$ . Before proceeding with numerical calculation, we need to make precise the value of  $Q$ . If we were considering the process  $gg \rightarrow C^0 g$ , where  $C^0$  is the  $U(1)$  gauge field tied to the  $U(3)$  brane, then  $Q = \sqrt{1/6}$  due to the normalization condition (6). However, for  $gg \rightarrow \gamma g$  there are two additional projections: from  $C_\mu$  to the hypercharge boson  $Y_\mu$ , giving a mixing factor  $\kappa$ ; and from  $Y_\mu$  onto a photon, providing an additional factor  $\cos \theta_W$  ( $\theta_W =$  Weinberg angle). The  $C^0 - Y$  mixing coefficient is model dependent: in the minimal model [6] it is quite small, around  $\kappa \simeq 0.12$  for couplings evaluated at the  $Z$  mass, which is modestly enhanced to  $\kappa \simeq 0.14$  as a result of RG running of the couplings up to 2.5 TeV. It should be noted that in models [7, 8] possessing an additional  $U(1)$  which partners  $SU(2)_L$  on a  $U(2)$  brane, the various assignment of the charges can result in values of  $\kappa$  which can differ considerably from 0.12. In what follows, we take as a fiducial value  $\kappa^2 = 0.02$ . Thus, if (20) is to describe  $gg \rightarrow \gamma g$ , we modify our definition of  $Q$  given in Eq. (5) to accommodate the additional mixings, and obtain

$$Q^2 = \frac{1}{6} \kappa^2 \cos^2 \theta_W \simeq 2.55 \times 10^{-3} \quad (\kappa^2/0.02) \quad . \tag{21}$$

In the remainder of the paper, we explore potential searches for Regge excitations of fundamental strings at LHC.

### III. ISOLATED HARD PHOTONS

In order to assess the possibility of discovery of signal above QCD background, we adopt the kind of signal introduced in [20] to study detection of TeV-scale black holes at the LHC, namely a high- $k_\perp$  isolated  $\gamma$  or  $Z$ . Thus, armed with parton distribution functions (CTEQ6D) [21] we have calculated integrated cross sections  $\sigma(pp \rightarrow \gamma + \text{jet})|_{k_\perp(\gamma) > k_{\perp,\min}}$  for both the background QCD processes (see Appendix I) and for  $gg \rightarrow \gamma g$ , for an array of values for the string scale  $M_s$  (see Appendix II). Our results are shown in Fig. 2. It is evident that the background is significantly reduced for large  $k_{\perp,\min}$ . At very large values of  $k_{\perp,\min}$ , however, event rates become problematic. In Fig. 3 we show the string cross

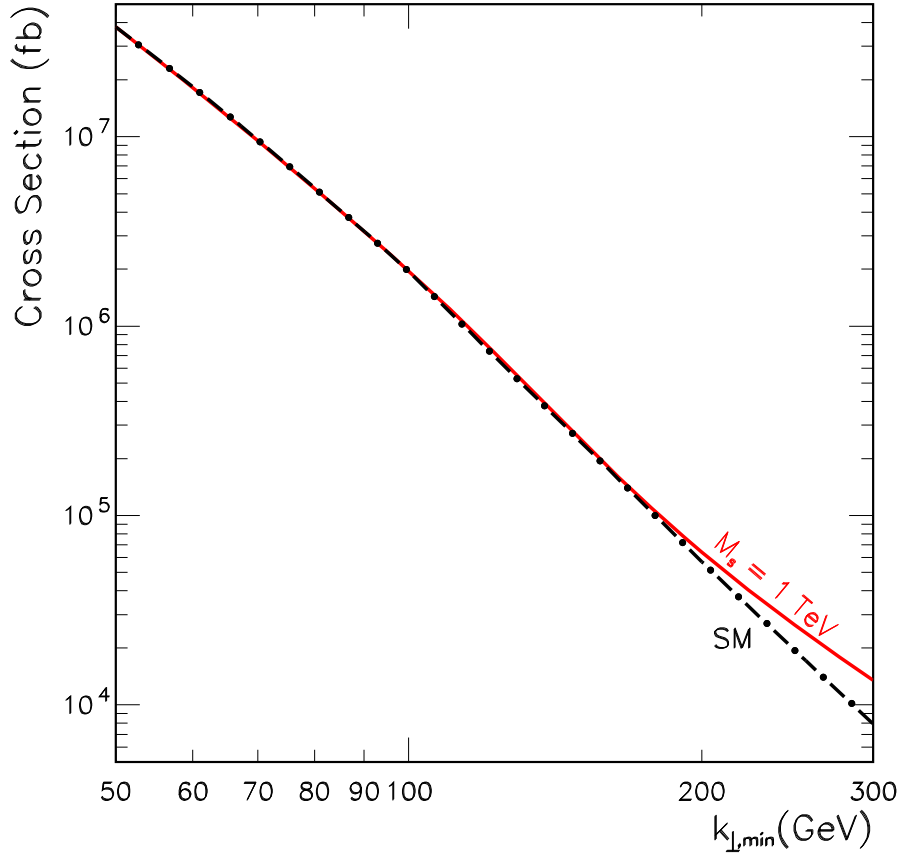


FIG. 2: Behavior of the QCD cross section for  $pp \rightarrow \gamma + \text{jet}$  (dot-dashed line) as a function of  $k_{\perp, \min}$ . The string cross section overlying the QCD background is also shown as a solid line, for  $M_s = 1 \text{ TeV}$ .

section and number of events (before cuts) in a  $100 \text{ fb}^{-1}$  run at LHC, for  $k_{\perp, \min} = 300 \text{ GeV}$ , as a function of the string scale  $M_s$ . Next, we explore the LHC discovery potential by computing the signal-to-noise ratio ( $\text{signal}/\sqrt{\text{SM background}} \equiv \text{S/N}$ ). For a  $300 \text{ GeV}$  cut in the transverse momentum, the QCD cross section (shown in Fig. 2) is about  $8 \times 10^3 \text{ fb}$ , yielding (for  $100 \text{ fb}^{-1}$ )  $\sqrt{\text{SM background}} \approx 895$ . A point worth noting at this juncture: to minimize misidentification with a high- $k_{\perp} \pi^0$ , isolation cuts must be imposed on the photon, and to trigger on the desired channel, the hadronic jet must be identified [22]. We will leave the exact nature of these cuts for the experimental groups, and present results for a generous range of direct photon reconstruction efficiency. To do so, we define the parameter

$$\beta = \frac{\text{background due to misidentified } \pi^0 \text{ after isolation cuts}}{\text{QCD background from direct photon production}} + 1. \quad (22)$$

Therefore, the noise is increased by a factor of  $\sqrt{\beta}$ , over the direct photon QCD contribution. Our significant results are encapsulated in Fig. 4, where we show the discovery reaches of the LHC for different integrated luminosities and  $\kappa^2 = 0.02$ . A detailed study of the CMS potential for isolation of prompt- $\gamma$ 's has been recently carried out [23], using GEANT4 simulations of  $\gamma + \text{jet}$  events generated with Pythia. This analysis (which also includes  $\gamma$ 's

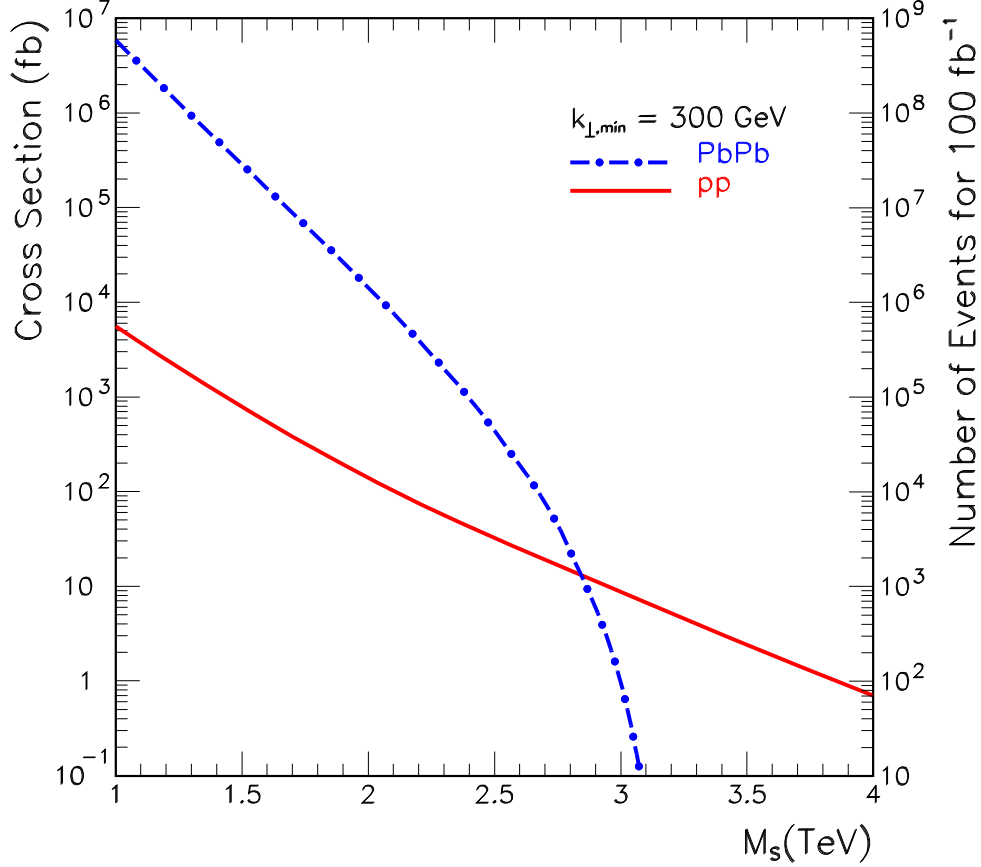


FIG. 3: Cross section for gluon fusion into  $\gamma + \text{jet}|_{k_{\perp}(\gamma) > 300 \text{ GeV}}$  and expected number of events, for  $100 \text{ fb}^{-1}$  and varying string scale.

produced in the decays of  $\eta$ ,  $K_s^0$ ,  $\omega^0$ , and bremsstrahlung photons emerging from high- $p_{\perp}$  jets) suggests  $\beta \simeq 2$ . Of course, considerations of detector efficiency further reduce the  $S/N$  ratio by an additional factor  $\epsilon$ , where  $1 < \epsilon \ll \sqrt{\beta}$ . We conclude that *discovery at the LHC would be possible for  $M_s$  as large as 2.3 TeV*. The dependence of the discovery reach with the  $C^0 - Y$  mixing coefficient  $\kappa$  has been extensively discussed in the accompanying Letter [4].

We now briefly explore the potential of ALICE to search for low mass string excitations [24]. With this motivation, we extend our analysis to include heavy ions collisions. In the spirit of Ref. [25] we consider the unshadowed parton distribution functions, i.e.,

$$R_{i/A}(x) = \frac{f_{i/A}(x, Q)}{Af_i(x, Q)} \simeq 1, \quad (23)$$

where  $f_{i/A}$  and  $f_i$  are the parton distribution functions inside a free nucleus of mass  $A$  and free nucleon, respectively. For  $M_s \gtrsim 1 \text{ TeV}$ , this approximation holds because LHC Pb-Pb collisions probe the minimum value of parton momentum at  $x_{\min} \approx M_s^2/s \sim 0.033$ , where there are no shadowing effects. A comparison of the string cross section for gluon fusion into  $\gamma + \text{jet}|_{k_{\perp}(\gamma) > 300 \text{ GeV}}$  for  $pp$  and Pb-Pb collisions is shown in Fig. 3. However, the larger aggregate of partons also increase the SM background; namely, for  $k_{\perp, \min} > 300 \text{ GeV}$ ,



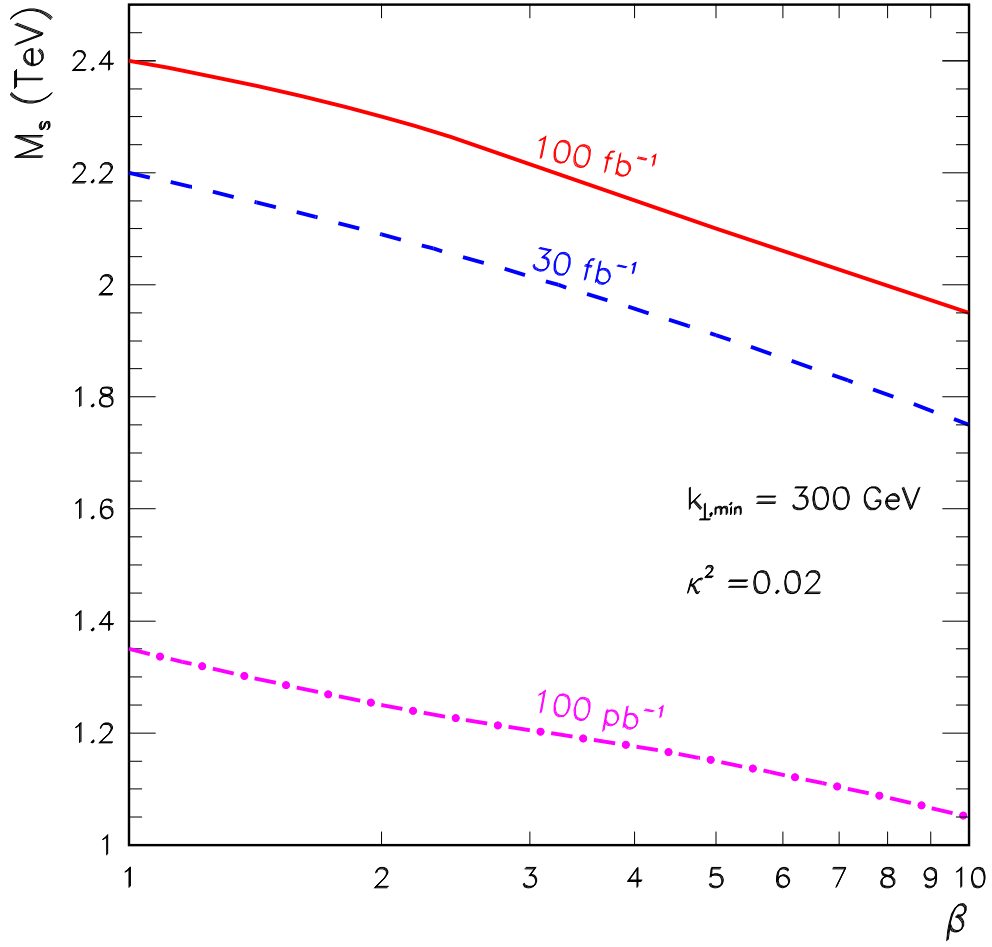


FIG. 4: Contours of  $5\sigma$  discovery in the  $(M_s, \text{detector efficiency})$  plane for different integrated luminosities and  $\kappa^2 = 0.02$ .

$\sigma_{\text{Pb-Pb} \rightarrow \gamma X} \approx 2.8 \times 10^7 \text{ fb}$ . This greatly decreases the sensitivity to D-brane models, which would require a Pb-Pb integrated luminosity of a few hundred  $\text{pb}^{-1}$ . This is substantially larger than the present day estimate [26].

#### IV. BUMP-HUNTING

The discovery trigger described in the previous section, the observation of isolated photons at large transverse momentum, serves very well as a signature of new physics. Given the particular nature of the process we are considering, the production of a TeV-scale resonance and its subsequent 2-body decay, signatures in addition to large  $k_\perp$  photons are available. Most apparently, one would hope that the resonance would be visible in data binned according to the invariant mass  $M$  of the photon + jet, setting cuts on photon and jet rapidities,  $y_1, y_2 < y_{\text{max}}$ , respectively. With the definitions  $Y \equiv \frac{1}{2}(y_1 + y_2)$  and  $y \equiv \frac{1}{2}(y_1 - y_2)$ , the

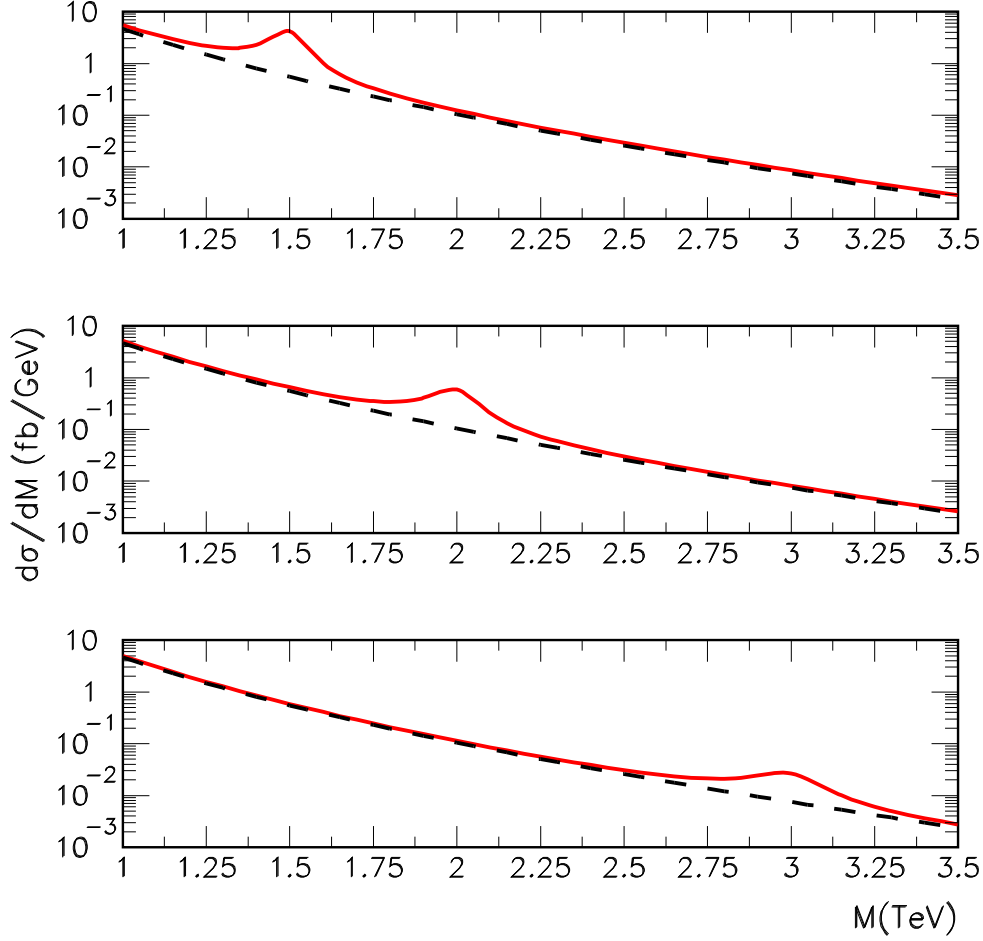


FIG. 5:  $d\sigma/dM$  (units of fb/GeV) *vs.*  $M$  (TeV) is plotted for the case of SM QCD background (dashed) and (first resonance) string signal + background (solid).

cross section per interval of  $M$  for  $pp \rightarrow \gamma + \text{jet} + X$  is given by [27]

$$\begin{aligned} \frac{d\sigma}{dM} = M\tau \sum_{ijk} & \left[ \int_{-Y_{\max}}^0 dY f_i(x_a, M) f_j(x_b, M) \int_{-(y_{\max}+Y)}^{y_{\max}+Y} dy \frac{d\sigma}{d\hat{t}} \Big|_{ij \rightarrow \gamma k} \frac{1}{\cosh^2 y} \right. \\ & \left. + \int_0^{Y_{\max}} dY f_i(x_a, M) f_j(x_b, M) \int_{-(y_{\max}-Y)}^{y_{\max}-Y} dy \frac{d\sigma}{d\hat{t}} \Big|_{ij \rightarrow \gamma k} \frac{1}{\cosh^2 y} \right] \end{aligned} \quad (24)$$

where  $i, j, k$  are different partons,  $\tau = M^2/s$ ,  $x_a = \sqrt{\tau}e^Y$ , and  $x_b = \sqrt{\tau}e^{-Y}$ . The kinematics of the scattering provides the relation

$$k_{\perp} = \frac{M}{2 \cosh y} \quad (25)$$

which, when combined with the standard cut  $k_{\perp} \gtrsim k_{\perp, \min}$ , imposes a *lower* bound on  $y$  to be implemented in the limits of integration. (For details see Appendix III.) The  $Y$  integration range in Eq. (24),  $Y_{\max} = \min\{\ln(1/\sqrt{\tau}), y_{\max}\}$ , comes from requiring  $x_a, x_b < 1$  together with the rapidity cuts  $|y_1|, |y_2| \leq 2.4$ . Finally, the Mandelstam invariants occurring in the cross section are given by  $\hat{s} = M^2$ ,  $\hat{t} = -\frac{1}{2}M^2 e^{-y}/\cosh y$ , and  $\hat{u} = -\frac{1}{2}M^2 e^{+y}/\cosh y$ .

In Fig. 5 we show several representative plots of this cross section for different values of  $M_s$ . Standard bump-hunting methods, such as calculating cumulative cross sections

$$\sigma(M_0) = \int_{M_0}^{\infty} \frac{d\sigma}{dM} dM \quad (26)$$

and searching for regions with significant deviations from the QCD background, may allow to find an interval of  $M$  suspected of containing a bump. With the establishment of such a region, one may calculate a signal-to-noise ratio, with the signal rate estimated in the invariant mass window  $[M_s - 2\Gamma, M_s + 2\Gamma]$ . This estimate of signal-to-noise would be roughly the same as that obtained through the inclusive cut  $k_{\perp} > 300$  GeV. This follows from the relation (25): for  $M$  in the range of  $M_s \gtrsim 2$  and for the significant contributing regions of  $y$ , the resulting  $k_{\perp}$  cut in Eq. (25) does not differ significantly from the 300 GeV [28]. Should bumps be found, the D-brane model can be further differentiated from other TeV-scale resonant processes by the details of the angular distributions inherent in Eq. (20).

## V. CONCLUDING DISCUSSION

In this work we have described how to search for the effects of Regge excitations of fundamental strings at LHC collisions. The underlying parton process for the excitation of the string resonance is dominantly the single photon production in gluon fusion,  $gg \rightarrow \gamma g$ , with open string states propagating in intermediate channels. If the photon mixes with the gauge boson of the baryon number, which is a common feature of D-brane quivers, the amplitude appears already at the string disk level. It is completely determined by the mixing parameter – and it is otherwise model-(compactification-) independent. We have shown that even for relatively small mixing, 100 fb<sup>-1</sup> of LHC data (in the  $pp \rightarrow \gamma + \text{jet}$  channel) could probe deviations from SM physics at a 5 $\sigma$  significance, for  $M_s$  as large as 2.3 TeV. We note that such a numerical value for the discovery reach is lower than the estimate presented in the accompanying Letter,  $M_s \sim 3.3$  TeV [4]. The present analysis contains a refined treatment of the resonance region, including the recently computed decay widths of both spin  $J = 0$  and spin  $J = 2$  Regge recurrence of the gluon octet [5]. The discovery reach is lower because these resonances are slightly wider than naïvely expected while the signal cross sections are very sensitive to the width values.

In closing we discuss some interesting contrast of  $\gamma$  and  $Z$  production that can serve as an additional marker of the D-brane model. Ignoring the  $Z$ -mass (i.e., keeping only transverse  $Z$ 's), and assuming that cross sections  $\times$  branching into lepton pairs are large enough for complete reconstruction to  $pp \rightarrow Z + \text{jet}$ , the quiver contribution to the signal is suppressed relative to the photon signal by a factor of  $\tan^2 \theta_W = 0.29$ . The SM ratio ( $Z$  background)/( $\gamma$  background) is roughly 0.92 for processes involving  $u$  (or  $\bar{u}$ ) quarks, and 4.7 for processes involving  $d$  (or  $\bar{d}$ ) quark. Thus, even if  $d$  quark processes are ignored, one obtains a signal-to-noise ratio  $(S/N)_Z = 0.29/\sqrt{0.92} = 0.30 (S/N_{\gamma})$ . Keeping the  $d$  quarks will only lead to more suppression of  $(S/N)_Z$  [29]. This implies that if the high- $k_{\perp}$  photons, as predicted by the TeV string model, are discovered at 5 $\sigma$ , they will not be accompanied by any significant deviation of  $pp \rightarrow Z + \text{jet}$  from SM predictions. This differs radically from the evaporation of black holes produced at the LHC. In such a case, production of high- $k_{\perp}$   $Z$  and  $\gamma$  are comparable. The suppression of high- $k_{\perp}$   $Z$  production, whose origin lies in the particular structure of the quiver model, will hold true for all the low-lying levels of the string.

## Acknowledgments

L.A.A. is supported by the U.S. National Science Foundation and the UWM Research Growth Initiative. H.G. is supported by the U.S. National Science Foundation Grants No PHY-0244507 and PHY-0757959. The research of T.R.T. is supported by the U.S. National Science Foundation Grants PHY-0600304, PHY-0757959 and by the Cluster of Excellence “Origin and Structure of the Universe” in Munich, Germany. He is grateful to Dieter Lüst and to Max-Planck-Institut für Physik, Werner-Heisenberg-Institut in Munich for their kind hospitality. Any opinions, findings, and conclusions or recommendations expressed in this material are those of the authors and do not necessarily reflect the views of the National Science Foundation.

## Appendix I

The SM background for processes with a single photon in the final state originates in the parton tree level processes  $gq \rightarrow \gamma q$ ,  $g\bar{q} \rightarrow \gamma\bar{q}$  and  $q\bar{q} \rightarrow \gamma g$ ,

$$2E' \frac{d\sigma}{d^3k'} \Big|_{pp \rightarrow \gamma X} = \sum_{ijk} \int dx_a dx_b f_i(x_a, Q) f_j(x_b, Q) 2E' \frac{d\hat{\sigma}}{d^3k'} \Big|_{ij \rightarrow \gamma k}, \quad (27)$$

where  $x_a$  and  $x_b$  are the fraction of momenta of the parent hadrons carried by the partons which collide,  $k'$  ( $E'$ ) is the photon momentum (energy),  $d\hat{\sigma}/d^3k'|_{ij \rightarrow \gamma k}$  is the cross section for scattering of partons of type  $i$  and  $j$  according to elementary QCD diagrams,  $f_i(x_a, Q)$  and  $f_j(x_b, Q)$  are parton distribution functions,  $Q$  is the momentum transfer, and the sum is over the parton species:  $g, q = u, d, s, c, b$ . In what follows we focus on  $gq \rightarrow \gamma q$ , which results in the dominant contribution to the total cross section. Corrections from the other two processes can be computed in a similar fashion. The hard parton-level cross section reads,

$$2E' \frac{d\hat{\sigma}}{d^3k'} \Big|_{gq \rightarrow \gamma q} = \frac{(2\pi)^4}{(2\pi)^6} \frac{1}{2\hat{s}} \delta[(k+p-k')^2] \frac{1}{4} \sum |\mathcal{M}|^2 = \frac{1}{(2\pi)^2} \frac{1}{2\hat{s}} \delta(2p \cdot q + q^2) \frac{1}{4} \sum |\mathcal{M}|^2, \quad (28)$$

where  $k$  and  $p$  are the momenta of the incoming partons,  $q = k - k'$ ,  $\hat{s} = x_a x_b s$ , and  $-q^2 = -\hat{t} = Q^2$ . Here,

$$\frac{1}{4} \sum |\mathcal{M}|^2 = \frac{1}{3} g^2 e^2 e_q^2 \left( \frac{\hat{s}}{\hat{s} + \hat{t}} + \frac{\hat{s} + \hat{t}}{\hat{s}} \right), \quad (29)$$

where  $g$  and  $e$  are the QCD and electromagnetic coupling constants, and  $e_q$  is the fractional electric charge of species  $q$ . For completeness we note that for  $q\bar{q} \rightarrow g\gamma$ ,

$$\frac{1}{4} \sum |\mathcal{M}|^2 = \frac{8}{9} g^2 e^2 e_q^2 \left( -\frac{\hat{t}}{\hat{s} + \hat{t}} - \frac{\hat{s} + \hat{t}}{\hat{t}} \right). \quad (30)$$

Equation (28) can be most conveniently integrated in terms of the rapidity  $y$  and transverse momentum  $k_\perp$  of the final photon

$$\frac{d^3k'}{2E'} = \frac{1}{2} d^2k_\perp dy = \pi k_\perp dk_\perp dy. \quad (31)$$

Considering that the incoming momentum of the gluon is  $k = x_a P_1$  and that of the quark is  $p = x_b P_2$ , we can re-write the argument of the delta function as

$$2p \cdot q + q^2 = 2x_b P_2 \cdot (x_a P_1 - k') + \hat{t} = x_a x_b s - 2x_b P_2 \cdot k' + \hat{t}, \quad (32)$$

where  $P_1$  and  $P_2$  are the initial momenta of the parent protons. Introducing,  $k'_0 = k_\perp \cosh y$ ,  $k'_\parallel = k_\perp \sinh y$ ,  $P_1 = (\sqrt{s}/2, 0, 0, \sqrt{s}/2)$ , and  $P_2 = (\sqrt{s}/2, 0, 0, -\sqrt{s}/2)$  we obtain

$$P_2 \cdot k' = \frac{\sqrt{s}}{2} k_\perp (\cosh y + \sinh y) = \frac{\sqrt{s}}{2} k_\perp e^y \quad (33)$$

and

$$\hat{t} = -2k \cdot k' = -2x_a \frac{\sqrt{s}}{2} k_\perp e^{-y} = -\sqrt{s} k_\perp e^{-y} x_a, \quad (34)$$

so that

$$\begin{aligned} \delta(x_a x_b s - \sqrt{s} x_b k_\perp e^y - \sqrt{s} x_a k_\perp e^{-y}) &= \frac{1}{s} \delta(x_a x_b - x_b x_\perp e^y - x_a x_\perp e^{-y}) \\ &= \frac{1}{s [x_a - x_\perp e^y]} \delta\left(x_b - \frac{x_a x_\perp e^{-y}}{x_a - x_\perp e^y}\right), \end{aligned} \quad (35)$$

where  $x_\perp = k_\perp/\sqrt{s}$ . The lower bound  $x_b > 0$  implies  $x_a > x_\perp e^y$ . The upper bound  $x_b < 1$  leads to a stronger constraint

$$x_a > \frac{x_\perp e^y}{1 - x_\perp e^{-y}}, \quad (36)$$

which requires  $x_\perp e^y < 1 - x_\perp e^{-y}$ , yielding  $x_\perp < (2 \cosh y)^{-1}$ . Of course there is another completely symmetric term, in which  $g$  comes from  $P_2$  and  $q$  comes from  $P_1$ . Putting all this together, the total contribution from  $gq \rightarrow \gamma q$  reads

$$\begin{aligned} \sigma_{pp \rightarrow \gamma X}^{qg \rightarrow \gamma q} &= 2 \sum_q \int \frac{d^3 k'}{2E'} \int dx_a \int dx_b f_g(x_a, Q) f_q(x_b, Q) \frac{1}{(2\pi)^2} \frac{1}{s [x_a - x_\perp e^y]} \\ &\times \frac{1}{2\hat{s}} \delta\left(x_b - \frac{x_a x_\perp e^{-y}}{x_a - x_\perp e^y}\right) \frac{e^2 g^2 e_q^2}{3} \left( \frac{\hat{s} + \hat{t}}{\hat{s}} + \frac{\hat{s}}{\hat{s} + \hat{t}} \right). \end{aligned} \quad (37)$$

With the change of variables  $z = e^y$  Eq. (37) can be re-written as

$$\begin{aligned} \sigma_{pp \rightarrow \gamma X}^{qg \rightarrow \gamma q} &= 2 \sum_q \int \frac{\pi k_\perp dk_\perp dz}{z} \int dx_a \int dx_b f_g(x_a, Q) f_q(x_b, Q) \frac{1}{(2\pi)^2 2x_a x_b s^2 (x_a - x_\perp z)} \\ &\times \delta\left(x_b - \frac{x_a x_\perp z^{-1}}{x_a - x_\perp z}\right) \frac{e^2 g^2 e_q^2}{3} \left( \frac{\hat{s} + \hat{t}}{\hat{s}} + \frac{\hat{s}}{\hat{s} + \hat{t}} \right). \end{aligned} \quad (38)$$

Now, since

$$\frac{\hat{t}}{\hat{s}} = -\frac{\sqrt{s} k_\perp e^{-y}}{x_b s} = -\frac{x_\perp}{x_b z} = \frac{x_\perp z}{x_a} - 1, \quad (39)$$

Eq. (38) becomes

$$\begin{aligned} \sigma_{pp \rightarrow \gamma X}^{qg \rightarrow \gamma q} &= \frac{e^2 g^2}{12\pi s} \int_{x_{\perp \min}}^{1/2} dx_\perp \int_{z_{\min}}^{z_{\max}} dz \int_{x_{a, \min}}^1 dx_a f_g(x_a, Q) \left[ \sum_q e_q^2 f_q\left(\frac{x_a x_\perp z^{-1}}{x_a - x_\perp z}, Q\right) \right] \\ &\times \frac{1}{x_a^2} \left( \frac{x_\perp z}{x_a} + \frac{x_a}{x_\perp z} \right), \end{aligned} \quad (40)$$

where the integration limits,

$$z_{\min}^{\max} = \frac{1}{2} \left[ \frac{1}{x_{\perp}} \pm \sqrt{\frac{1}{x_{\perp}^2} - 4} \right] \quad \text{and} \quad x_{a,\min} = \frac{x_{\perp} z}{1 - x_{\perp} z^{-1}}, \quad (41)$$

are obtained from Eq. (36). In Fig. 2 we show the QCD background cross section *vs*  $k_{\perp,\min}$ , as obtained through numerical integration of Eq. (40). To accommodate the minimal acceptance cuts on final state photons from the CMS and ATLAS proposals [30], an additional kinematic cut,  $|y| < 2.4$ , has been included in the calculation.

## Appendix II

For the considerations in the present work, the resonant cross section can be safely approximated by single poles in the Narrow-Width Approximation,

$$\frac{\Gamma\sqrt{s_0}/\pi}{(\hat{s} - s_0)^2 + (\Gamma\sqrt{s_0})^2} \frac{\pi}{\Gamma\sqrt{s_0}} = \frac{\pi}{\Gamma\sqrt{s_0}} \delta(\hat{s} - s_0), \quad (42)$$

where  $s_0 = M_s^2$ . The scattering proceeds through  $J = 0$  and  $J = 2$  angular momentum states, with the  $M_s^8$  term in Eq. (20) originating from  $J = 0$ , and the  $t^4 + u^4$  piece reflecting  $J = 2$  activity. The widths of these two resonances are different, with  $\Gamma^{J=0} = (3/4)\alpha_s M_s$ , and  $\Gamma^{J=2} = (9/20)\alpha_s M_s$  [5]. The average string amplitude square in Eq. (20) then becomes

$$\begin{aligned} |\mathcal{M}(gg \rightarrow g\gamma)|^2 &\approx 4g^4 Q^2 C(N) \frac{\pi}{s_0^{5/2}} \left[ \frac{s_0^4}{\Gamma^{J=0}} + \frac{\hat{t}^4 + (\hat{t} + s_0)^4}{\Gamma^{J=2}} \right] \delta(\hat{s} - s_0) \\ &= 4g^4 Q^2 C(N) \frac{\pi}{\alpha_s s_0^3} \left\{ \frac{4}{3}s_0^4 + \frac{20}{9}[\hat{t}^4 + (\hat{t} + s_0)^4] \right\} \delta(\hat{s} - s_0). \end{aligned} \quad (43)$$

Thus, the total cross section for single photon production in gluon fusion is given by

$$\begin{aligned} \sigma_{pp \rightarrow \gamma g}^{gg \rightarrow \gamma g} &= \int \frac{d^3 k'}{2E'} \int dx_a \int dx_b f_g(x_a, Q) f_g(x_b, Q) \frac{1}{(2\pi)^2} \frac{1}{2\hat{s}s} \delta(x_a x_b - x_b x_{\perp} z - x_a x_{\perp} z^{-1}) \\ &\times 4g^4 Q^2 C(N) \frac{\pi}{\alpha_s s_0^3} \left\{ \frac{4}{3}s_0^4 + \frac{20}{9}[\hat{t}^4 + (\hat{t} + s_0)^4] \right\} \delta(\hat{s} - s_0). \end{aligned} \quad (44)$$

We set  $Q = M_s$ , which is appropriate for the dual picture of string theory. We are aware that for  $Q \sim M_s$ , the parton distribution functions will receive significant corrections from the rapid increase of degrees of freedom. Fortunately, as noted elsewhere [31], at parton center-of-mass energies corresponding to low-lying string excitations the resonant cross section is largely insensitive to the details of the choice of  $Q$ . Plugging  $\tau_0 = s_0/s$  into Eq. (44), we obtain

$$\begin{aligned} \sigma_{pp \rightarrow \gamma g}^{gg \rightarrow \gamma g} &= \int \frac{\pi k_{\perp} dk_{\perp} dz}{z} \int dx_a \int dx_b f_g(x_a, Q) f_g(x_b, Q) \frac{\delta(x_a x_b - x_b x_{\perp} z - x_a x_{\perp} z^{-1})}{8\pi^2 x_a^2 x_b} \\ &\times 4g^4 Q^2 C(N) \frac{\pi s}{\alpha_s s_0^3} \left\{ \frac{4}{3}\tau_0^4 + \frac{20}{9}[(x_a x_{\perp} z^{-1})^4 + (-x_a x_{\perp} z^{-1} + \tau_0)^4] \right\} \\ &\times \delta\left(x_b - \frac{\tau_0}{x_a}\right), \end{aligned} \quad (45)$$

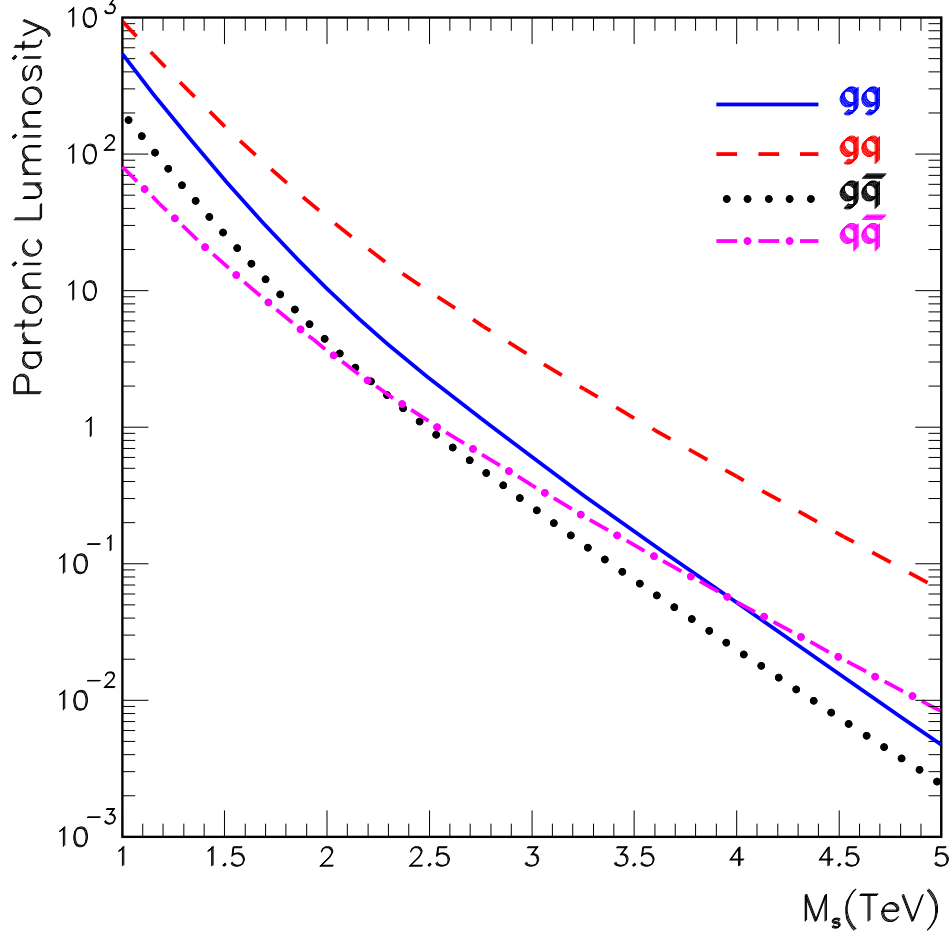


FIG. 6: Relative contributions of initial state partons ( $ij = gg, qq, g\bar{q}$ , and  $q\bar{q}$ ) to  $\int_{\tau_0}^1 f_i(x_a, Q) f_j(\tau_0/x_a, Q) dx_a/x_a$ , with varying string scale.

which after integration over  $x_b$  leads to

$$\sigma_{pp \rightarrow \gamma X}^{gg \rightarrow \gamma g} = \frac{g^4 Q^2 C(N)}{2 \alpha_s \tau_0^4 s} \int \frac{x_\perp dx_\perp dz}{z} \int dx_a f_g(x_a, Q) f_g(\tau_0/x_a, Q) \frac{1}{x_a} \times \delta \left( \tau_0 - \frac{\tau_0 x_\perp z}{x_a} - \frac{x_a x_\perp}{z} \right) \left\{ \frac{4}{3} \tau_0^4 + \frac{20}{9} [(x_a x_\perp z^{-1})^4 + (-x_a x_\perp z^{-1} + \tau_0)^4] \right\}. \quad (46)$$

We now make use of the delta function scaling property,

$$\delta \left( \tau_0 - \frac{\tau_0 x_\perp z}{x_a} - \frac{x_\perp x_a}{z} \right) = \delta(f(z)) = \frac{1}{|f'(z_+)|} \delta(z - z_+) + \frac{1}{|f'(z_-)|} \delta(z - z_-), \quad (47)$$

where  $z_\pm$  are the solutions to  $f(z) = 0$ ,

$$z_\pm = \frac{x_a}{2x_\perp} \left( 1 \pm \sqrt{1 - \frac{4x_\perp^2}{\tau_0}} \right). \quad (48)$$

Besides,

$$\frac{1}{z_{\pm}|f'(z_{\pm})|} = \left| \frac{\tau_0 x_{\perp} z_{\pm}}{x_a} - \frac{x_a x_{\perp}}{z_{\pm}} \right|^{-1} \quad (49)$$

and

$$\frac{x_a x_{\perp}}{z_{\pm}} = \frac{\tau_0}{2} \left( 1 \mp \sqrt{1 - \frac{4x_{\perp}^2}{\tau_0}} \right); \quad (50)$$

therefore,

$$\frac{1}{z_{\pm}|f'(z_{\pm})|} = \frac{1}{\tau_0 \sqrt{1 - 4x_{\perp}^2/\tau_0}}. \quad (51)$$

A straightforward calculation shows that

$$\begin{aligned} \frac{16}{9} \tau_0^2 (5 x_{\perp}^4 - 10 x_{\perp}^2 \tau_0 + 4 \tau_0^2) &= \left\{ \frac{4}{3} \tau_0^4 + \frac{20}{9} [(x_a x_{\perp} z_+^{-1})^4 + (-x_a x_{\perp} z_+^{-1} + \tau_0)^4] \right\} \\ &+ \left\{ \frac{4}{3} \tau_0^4 + \frac{20}{9} [(x_a x_{\perp} z_-^{-1})^4 + (-x_a x_{\perp} z_-^{-1} + \tau_0)^4] \right\}, \end{aligned} \quad (52)$$

and hence integration over the  $z$  variable yields

$$\begin{aligned} \sigma_{pp \rightarrow \gamma X}^{gg \rightarrow \gamma g} &= \frac{8}{9} \frac{g^4 Q^2 C(N)}{\alpha_s \tau_0^3 s} \int_{x_{\perp, \min}}^{\sqrt{\tau_0}/2} dx_{\perp} \frac{x_{\perp}}{\sqrt{1 - 4x_{\perp}^2/\tau_0}} (5 x_{\perp}^4 - 10 x_{\perp}^2 \tau_0 + 4 \tau_0^2) \\ &\times \int_{\tau_0}^1 \frac{dx_a}{x_a} f_g(x_a, Q) f_g(\tau_0/x_a, Q), \end{aligned} \quad (53)$$

where the integration range has been derived from the conditions  $0 < x_b = \tau_0/x_a < 1$  and  $4x_{\perp}^2 < \tau_0$ , which imply  $\tau_0 < x_a < 1$  and  $x_{\perp, \min} < x_{\perp} < \sqrt{\tau_0}/2$ . Finally, integration over  $x_{\perp}$  leads to

$$\begin{aligned} \sigma_{pp \rightarrow \gamma X}^{gg \rightarrow \gamma g} &= \frac{1}{9} \frac{g^4 Q^2 C(N)}{\alpha_s \tau_0^2 s} \sqrt{1 - \frac{4x_{\perp, \min}^2}{\tau_0}} (5 \tau_0^2 - 6 \tau_0 x_{\perp, \min}^2 + 2 x_{\perp, \min}^4) \\ &\times \int_{\tau_0}^1 \frac{dx_a}{x_a} f_g(x_a, Q) f_g(\tau_0/x_a, Q). \end{aligned} \quad (54)$$

Note that all stringy corrections to the pure bosonic cross section given by Eq. (54) have similar factorizations. An illustration of the relative partonic luminosities of the different processes is shown in Fig. 6.

### Appendix III

We follow the same conventions and notation given in Appendix I for two-body processes leading to final states consisting of  $\gamma$  + jet, with equal and opposite transverse momenta  $k_{\perp}$  and  $p_{\perp}$ , respectively. The distribution of invariant masses  $M^2 = (k' + p')^2$  is given by

$$\begin{aligned} \frac{d\sigma}{dM^2} &= \frac{(2\pi)^4}{(2\pi)^6} \int \frac{d^3 k'}{2E'_1} \int \frac{d^3 p'}{2E'_2} \sum_{ijk} \int dx_a \int dx_b f_i(x_a, M) f_j(x_b, M) \delta^4(p - k' - p') \\ &\times \delta(p^2 - M^2) \frac{1}{2\widehat{s}} \sum_{\text{spins}} |\mathcal{M}|^2, \end{aligned} \quad (55)$$



where

$$\sum_{\text{spins}} |\overline{\mathcal{M}}|^2 = |\mathcal{M}(ij \rightarrow \gamma k)|^2 = 64\pi^2 \widehat{s} \frac{d\sigma}{d\Omega} = 16\pi \widehat{s}^2 \left. \frac{d\sigma}{d\widehat{t}} \right|_{ij \rightarrow \gamma k}, \quad (56)$$

$p^2 = \widehat{s} = (k' + p')^2 = 2k' \cdot p' = 2E'_1 E'_2 - k'_\parallel p'_\parallel + p_\perp^2$ , and

$$\delta^4(p - k'_\perp - p'_\perp) = \delta(E - E_1 - E_2) \delta(p_\parallel - k'_\parallel - p'_\parallel) \delta(\vec{k}_\perp + \vec{p}_\perp). \quad (57)$$

The integration over  $d^3k' d^3p'$  can be conveniently re-written in terms of rapidities  $y_1$  and  $y_2$  (of the  $\gamma$  and the jet) and their common transverse momentum,

$$\frac{d^3p}{2E} = \frac{\pi}{2} dp_\perp^2 dy, \quad (58)$$

where  $y \equiv \frac{1}{2}(y_1 - y_2)$ . Since  $E'_1 = p_\perp \cosh y_1$ ,  $k'_\parallel = p_\perp \sinh y_1$ ,  $E'_2 = p_\perp \cosh y_2$ , and  $p'_\parallel = p_\perp \sinh y_2$ , a straightforward calculation leads to  $E'_1 E'_2 - k'_\parallel p'_\parallel = p_\perp^2 \cosh(y_1 - y_2) \equiv p_\perp^2 \cosh 2y$ . Now, using the identity of hyperbolic functions,  $1 + \cosh 2y = 2 \cosh^2 y$ , we define

$$\tau = \frac{\widehat{s}}{s} = \frac{M^2}{s} = \frac{4p_\perp^2}{s} \cosh^2 y \quad (59)$$

so that

$$\delta(\widehat{s} - M^2) = \delta(4p_\perp^2 \cosh^2 y - M^2) = \frac{1}{4 \cosh^2 y} \delta\left(p_\perp^2 - \frac{M^2}{4 \cosh^2 y}\right). \quad (60)$$

Using

$$\int d^2\vec{k}_\perp d^2\vec{p}_\perp \delta(\vec{k}_\perp + \vec{p}_\perp) \delta(p_\perp^2 - M^2/4 \cosh^2 y) = \pi \int dp_\perp^2 \delta(p_\perp^2 - M^2/4 \cosh^2 y) = \pi, \quad (61)$$

Eq. (55) becomes

$$\begin{aligned} \frac{d\sigma}{dM^2} &= \frac{\pi}{(2\pi)^2} \frac{1}{4} (8\pi M^2) \int dy_1 \int dy_2 \sum_{ijk} \int dx_a \int dx_b f_i(x_a, M) f_j(x_b, M) \frac{1}{4 \cosh^2 y} \\ &\times \delta(E - E'_1 - E'_2) \delta(p_\parallel - k'_\parallel - p'_\parallel) \left. \frac{d\sigma}{d\widehat{t}} \right|_{ij \rightarrow \gamma k}. \end{aligned} \quad (62)$$

We now define  $a = E - E_1 - E_2$  and  $b = p_\parallel - k'_\parallel - p'_\parallel$  to perform the change of variables  $A = a + b$  and  $B = a - b$ , such that  $\delta(a)\delta(b) = N\delta(A)\delta(B)$ , with normalization  $N$  given by

$$\int da db \delta(a) \delta(b) = \int dA dB \frac{\partial(a, b)}{\partial(A, B)} N \delta(A) \delta(B) = \frac{N}{2} = 1. \quad (63)$$

The new variables can then be explicitly written as  $\{A_B\} = E \pm p_\parallel - (E_1 \pm k'_\parallel) - (E_2 \pm p'_\parallel)$ , where  $E \pm p_\parallel = \left\{ \frac{\sqrt{s}x_a}{\sqrt{s}x_b} \right\}$ ,  $E_1 \pm k'_\parallel = p_\perp e^{\pm y_1} = p_\perp e^{\pm(Y+y)}$ , and  $E_2 \pm p'_\parallel = p_\perp e^{\pm y_2} = p_\perp e^{\pm(Y-y)}$ , with  $Y = \frac{1}{2}(y_1 + y_2)$ . Putting all this together, the product of delta functions in Eq. (62) becomes

$$\begin{aligned} \delta(E - E_1 - E_2) \delta(p_\parallel - k'_\parallel - p'_\parallel) &= 2\delta(\sqrt{s}x_a - 2p_\perp e^Y \cosh y) \delta(\sqrt{s}x_b - 2p_\perp e^{-Y} \cosh y) \\ &= 2\delta(\sqrt{s}x_a - M e^Y) \delta(\sqrt{s}x_b - M e^{-Y}), \end{aligned} \quad (64)$$

and hence integration over the fraction of momenta is straightforward, yielding

$$\frac{d\sigma}{dM} = \frac{1}{2} M \tau \int dy_1 dy_2 \frac{1}{\cosh^2 y} \sum_{ijk} f_i(\sqrt{\tau} e^Y, M) f_j(\sqrt{\tau} e^{-Y}, M) \left. \frac{d\sigma}{d\hat{t}} \right|_{ij \rightarrow \gamma k}. \quad (65)$$

Now, if we constrain the rapidities to the interval  $2.4 < y_1, y_2 < 2.4$  we obtain the invariant mass spectrum given in Eq. (24). In addition, note that  $x_a, x_b < 1$ , implying  $-\ln(1/\sqrt{\tau}) < Y < \ln(1/\sqrt{\tau})$ . Besides, the cut on the transverse momentum leads to  $k_{\perp, \min} < M/2 \cosh y$ . Finally, the Jacobian reads

$$dy_1 dy_2 = \frac{\partial(y_1, y_2)}{\partial(Y, y)} dY dy = 2 dY dy, \quad (66)$$

and the region of integration is defined by  $|y_1| = |y + Y| < 2.4$  and  $|y_2| = |y - Y| < 2.4$ .

- 
- [1] J. Polchinski, *String Theory*, Cambridge University Press (1998)
  - [2] For a recent review, see: R. Blumenhagen, B. Kors, D. Lüst and S. Stieberger, Phys. Rept. **445**, 1 (2007) [arXiv:hep-th/0610327].
  - [3] I. Antoniadis, N. Arkani-Hamed, S. Dimopoulos and G. R. Dvali, Phys. Lett. B **436**, 257 (1998) [arXiv:hep-ph/9804398]. For early work, see J.D. Lykken, Phys. Rev. D **54**, 3693 (1996) [arXiv:hep-th/9603133]
  - [4] L. A. Anchordoqui, H. Goldberg, S. Nawata and T. R. Taylor, Phys. Rev. Lett. **100**, 171603 (2008) [arXiv:0712.0386 [hep-ph]].
  - [5] L. A. Anchordoqui, H. Goldberg, and T. R. Taylor, arXiv:0806.3420 [hep-ph].
  - [6] D. Berenstein and S. Pinansky, Phys. Rev. D **75**, 095009 (2007) [arXiv:hep-th/0610104].
  - [7] I. Antoniadis, E. Kiritsis and T. N. Tomaras, Phys. Lett. B **486**, 186 (2000) [arXiv:hep-ph/0004214].
  - [8] R. Blumenhagen, B. Kors, D. Lüst and T. Ott, Nucl. Phys. B **616**, 3 (2001) [arXiv:hep-th/0107138].
  - [9] Stringy corrections to  $e^+e^- \rightarrow \gamma\gamma$  and  $e^+e^- \rightarrow e^+e^-$  were considered by S. Cullen, M. Perelstein and M. E. Peskin, Phys. Rev. D **62**, 055012 (2000) [arXiv:hep-ph/0001166].
  - [10] P. Burikham, T. Figy and T. Han, Phys. Rev. D **71**, 016005 (2005) [Erratum-ibid. D **71**, 019905 (2005)] [arXiv:hep-ph/0411094]; K. Cheung and Y. F. Liu, Phys. Rev. D **72**, 015010 (2005) [arXiv:hep-ph/0505241].
  - [11] P. Meade and L. Randall, arXiv:0708.3017 [hep-ph].
  - [12] For an earlier discussion of experimental signatures at LHC related to TeV strings, see G. Domokos and S. Kovesi-Domokos, Phys. Rev. Lett. **82**, 1366 (1999) [arXiv:hep-ph/9812260].
  - [13] L. A. Anchordoqui, H. Goldberg, D. Lüst, S. Nawata, S. Stieberger and T. R. Taylor, in preparation.
  - [14] S. J. Parke and T. R. Taylor, Phys. Rev. Lett. **56**, 2459 (1986).
  - [15] S. Stieberger and T. R. Taylor, Phys. Rev. D **74**, 126007 (2006) [arXiv:hep-th/0609175].
  - [16] S. Stieberger and T. R. Taylor, Phys. Rev. Lett. **97**, 211601 (2006) [arXiv:hep-th/0607184].
  - [17] M. L. Mangano and S. J. Parke, Phys. Rept. **200**, 301 (1991) [arXiv:hep-th/0509223].
  - [18] L. J. Dixon, arXiv:hep-ph/9601359.

- [19] T. van Ritbergen, A. N. Schellekens and J. A. M. Vermaseren, *Int. J. Mod. Phys. A* **14**, 41 (1999) [arXiv:hep-ph/9802376].
- [20] S. Dimopoulos and G. L. Landsberg, *Phys. Rev. Lett.* **87**, 161602 (2001) [arXiv:hep-ph/0106295].
- [21] J. Pumplin, D. R. Stump, J. Huston, H. L. Lai, P. Nadolsky and W. K. Tung, *JHEP* **0207**, 012 (2002) [arXiv:hep-ph/0201195].
- [22] See e.g., D. V. Bandurin and N. B. Skachkov, *Eur. Phys. J. C* **37**, 185 (2004);
- [23] P. Gupta, B. C. Choudhary, S. Chatterji, S. Bhattacharya and R. K. Shivpuri, arXiv:0705.2740 [hep-ex].
- [24] Pb-Pb  $\rightarrow \gamma + \text{jet}$  events can be identified by selecting a prompt photon and searching for the leading particle in the opposite direction inside the ALICE central tracking system. As photons emerge almost unaltered from dense medium, they provide a measurement of the original energy of the parton emitted in the opposite direction. G. Conesa, H. Delagrange, J. Diaz, Y. V. Kharlov and Y. Schutz, *Nucl. Instrum. Meth. A* **585**, 28 (2008) [arXiv:0711.2431 [physics.data-an]].
- [25] A. Chamblin and G. C. Nayak, *Phys. Rev. D* **66**, 091901 (2002) [arXiv:hep-ph/0206060].
- [26] A. Dainese, *J. Phys. G* **35**, 044046 (2008) [arXiv:0710.3052 [nucl-ex]].
- [27] E. Eichten, I. Hinchliffe, K. D. Lane and C. Quigg, *Rev. Mod. Phys.* **56**, 579 (1984) [Addendum-ibid. **58**, 1065 (1986)].
- [28] For  $M_s < 1.5$  TeV, the second resonance of the string mass spectrum ( $\sqrt{n}M_s$ ,  $n = 1, 2, \dots$ ) may be observed at the LHC in the  $pp \rightarrow \gamma + \text{jet}$  channel as well.
- [29] It is worth pausing to note that  $\pi^0$  misidentification does not play a role in the  $Z$  channel, and so this tends to decrease the QCD background. On the other hand, the string signal will suffer some suppression because of finite mass effects. These systematics (which have opposite effects on  $(S/N)_Z$ ) were not considered in the preceding discussion.
- [30] G. L. Bayatian *et al.* [CMS Collaboration], *J. Phys. G* **34** 995 (2007); W. W. Armstrong *et al.* [ATLAS Collaboration], CERN/LHCC 94-43.
- [31] L. A. Anchordoqui, J. L. Feng, H. Goldberg and A. D. Shapere, *Phys. Rev. D* **65** (2002) 124027 [arXiv:hep-ph/0112247].